Dedicator of Cytokinesis 5 Regulates Keratinocyte Function and Promotes Diabetic Wound Healing

Hua Qu,[1] Tian Miao,[1,2] Yuren Wang,[1] Liang Tan,[3,4] Bangliang Huang,[1] Linlin Zhang,[1] Xiufei Liu,[1] Min Long,[1] Rui Zhang,[1] Xiaoyu Liao,[1] Xiaoli Gong,[1] Ju Wang,[3] Xin Xiong,[1] Junli Liu,[5] Xi Li,[6] Jiang Yu,[7] Gangyi Yang,[8] Zhiming Zhu,[9] Hongting Zheng,[1] and Yi Zheng[1]

Diabetes 2021;70:1170–1184 | https://doi.org/10.2337/db20-1008

Cutaneous wound healing is a fundamental biologic and coordinated process, and failure to maintain this process contributes to the dysfunction of tissue homeostasis, increasing the global burden of diabetic foot ulcerations. However, the factors that mediate this process are not fully understood. Here, we identify the pivotal role of dedicator of cytokinesis 5 (Dock5) in keratinocyte functions contributing to the process of skin wound healing. Specifically, Dock5 is highly upregulated during the proliferative phase of wound repair and is predominantly expressed in epidermal keratinocytes. It regulates keratinocyte adhesion, migration, and proliferation and influences the functions of extracellular matrix (ECM) deposition by facilitating the ubiquitination of transcription factor ZEB1 to activate laminin-332/integrin signaling. Genetic ablation of Dock5 in mice leads to attenuated reepithelialization and granulation tissue formation, and Dock5 overexpression–improved skin repair can be abrogated by LAMA3 knockdown. Importantly, Dock5 expression in the skin edge is reduced in patients and animal models of diabetes, further suggesting a direct correlation between its abundance and healing capability. The rescue of Dock5 expression in diabetic mice causes a significant improvement in reepithelialization, collagen deposition, ECM production, and granulation. Our study provides a potential therapeutic target for wound healing impairment during diabetes.

COMPLICATIONS

The skin, as the body's external epithelium, sustains and repairs injuries throughout a lifetime. Cutaneous wound healing is a fundamental biologic and coordinated process that can be divided into four overlapping phases, including hemostasis, inflammation, proliferation, and remodeling. Each stage is characterized by key molecular, cellular, and physiologic events, which are orchestrated in large part by signaling among hematopoietic, immunologic, and resident skin cells (1). Immediately after injury, local vascular smooth muscle cells act to constrict vessels to reduce blood flow. Inflammation is then initiated within hours, and neutrophils and monocytes play their roles in succession to pave the way for the coming proliferative phase. In this intermediate stage, a series of actions, including keratinocyte migration and proliferation and extracellular matrix (ECM) deposition, occur to form

[1]Translational Research of Diabetes Key Laboratory of Chongqing Education Commission of China, Department of Endocrinology, Second Affiliated Hospital of Army Medical University, Chongqing, China
[2]Department of Respiratory and Critical Care Medicine, General Hospital of Western Theater Command, Chengdu, China
[3]Department of Neurosurgery, Southwest Hospital, Army Medical University, Chongqing, China
[4]Department of Electrical and Computer Engineering, Faculty of Science and Technology, University of Macau, Macau, China
[5]Shanghai Diabetes Institute, Department of Endocrinology and Metabolism, Shanghai Jiao Tong University Affiliated Sixth People's Hospital, Shanghai Jiao Tong University School of Medicine, Shanghai, China
[6]Biology Science Institutes, Chongqing Medical University, Chongqing, China
[7]Department of Outpatient, Second Affiliated Hospital of Army Medical University, Chongqing, China
[8]Department of Endocrinology, Second Affiliated Hospital of Chongqing Medical University, Chongqing, China
[9]Department of Hypertension and Endocrinology, Third Affiliated Hospital of Army Medical University, Chongqing, China

Corresponding authors: Yi Zheng, cecilia.zy@163.com, and Hongting Zheng, fnf7703@hotmail.com

Received 7 October 2020 and accepted 12 February 2021

Clinical trial reg. no. ChiCTR-ROC-17010719, http://www.chictr.org.cn

This article contains supplementary material online at https://doi.org/10.2337/figshare.13952456.

H.Q., T.M., Y.W., and L.T. contributed equally to this work.

granulation tissue. Last, in the collagen-remodeling phase, a scar is produced through type I collagen synthesis.

During the proliferative phase, reepithelialization, mainly achieved by epidermal cell migration and proliferation, is vital for rebuilding the continuity of the epidermal barrier (2). Almost 95% of the epidermis is composed of keratinocytes (3), and the basal keratinocytes are anchored to the basement membrane (BM) (separating the epidermis from the dermis) through specific ECM components binding integrins (4). The distinct cell behaviors evoked by these ECM-integrin complexes are not only essential for wound reepithelialization to restore epidermal homeostasis, but also influential in inflammatory response, ECM remodeling, and granulation tissue formation, facilitating proliferation and the transition from the proliferative to the remodeling phase (5,6). Dysfunctions of epidermal keratinocytes are often seen under diabetic conditions, leading to impaired wound healing and contributing to the pathophysiology of diabetic foot ulcers (DFUs). In patients with diabetes, the lifetime risk of developing DFUs, which cause limb amputation every 30 s worldwide and represent a major economic burden in health care management, is as high as 25% (7). Despite the magnitude of these consequences, an insufficient understanding of the underlying molecular mechanisms hampers the development of novel therapeutic strategies for diabetic wounds.

Dedicator of cytokinesis 5 (Dock5) is one of the candidate molecules known to be implicated in protein-protein interactions in various tissues through three domains (SH3, DHR1, and DHR2) (8), which are fundamental for multiple cellular responses, including myoblast fusion (9), bone resorption (10), and mast cell degranulation (11). Recently, Dock5 was reported to regulate hepatic insulin sensitivity (12) and participate in cell motility in head and neck squamous carcinoma (13). These findings raise questions about the possible role of Dock5 in skin homeostasis during wound healing.

In the current study, we uncovered a novel role of Dock5 in enhancing cellular processes, including adhesion, migration, and proliferation, as well as its capability of influencing ECM deposition during the proliferative phase, indicating that Dock5 may be a potential therapeutic target for ameliorating cutaneous wound repair impairment. In addition, activation of the Dock5-LAMA3 signaling pathway in skin may represent a new mechanism for treating DFUs.

RESEARCH DESIGN AND METHODS

Animals

Male C57BL/6, type 2 diabetes C57BL/KsJm/Leptdb (db/db) mice and their normoglycemic heterozygous littermates were purchased from the Model Animal Research Center of Nanjing University (Jiangsu, China). Dr. Cote (Burnham Institute for Medical Research, La Jolla, CA) generously provided Dock5 knockout (KO) mice, which were generated as previously reported (9) and backcrossed onto a C57BL/6 background for more than eight generations before use, and age- and sex-matched C57BL/6 mice were used as wild-type (WT) controls. $Dock5^{flox/flox}$ and keratin14-Cre mice were purchased from GemPharmatech (Jiangsu, China). Keratinocyte-specific Dock5 KO mice were generated by crossing $Dock5^{flox/flox}$ with keratin14-Cre mice, which express a Cre recombinase transgene under the control of a human keratin14 promoter as previously described (14), and Cre^{+} $Dock5^{WT/WT}$ mice were used as controls. Animals were 8–12 weeks old at the start of wounding after anesthetization with pentobarbital sodium. Mice were housed in a 12-h dark/light cycle at 22°C with food and water ad libitum. All mouse study designs, experimental processes, and euthanasia methods were approved by the Laboratory Animal Welfare and Ethics Committee of the Army Medical University.

Skin Wound Models

The wound model was deployed as previously described (15). Briefly, after general anesthesia, two full-thickness wounds were made on the dorsum on each side of the midline using a sterile 6-mm biopsy punch (HealthLink, Jacksonville, FL). Digital images were obtained on the day of surgery and every other day after wounding. Wound area was quantified using ImageJ software (National Institutes of Health, Bethesda, MD) with a unified calibration. The wound closure rate was calculated as the percentage of the original area. For the histology and mRNA and protein expression analysis during the wound healing process, mice were euthanized on the indicated day, and wound tissues were harvested using an 8-mm skin biopsy punch.

Quantitative Real-time PCR

Quantitative real-time PCR was performed according to our previous protocol (16). Briefly, total RNA was extracted from skin tissues or cultured cells using Trizol (TIANGEN, Beijing, China) according to the manufacturer's instructions. RNA quality was assessed by examining the 260:280 ratio using the NanoDrop2000 spectrophotometer (Thermo Scientific, Waltham, MA). Samples with a ratio of 1.8–2.0 were processed for further analysis. cDNA was obtained by reverse transcribing total RNA with the PrimeScript RT Reagent Kit (TaKaRa, Dalian, China). Quantitative real-time PCR was performed on the Applied Biosystems 7300 system (Life Technologies, Warrington, U.K.) using SYBR Premix Ex Taq II (TaKaRa). The internal control was GAPDH, and gene expression levels were calculated using the ΔCt method. The primer sequences are presented in Supplementary Table 1.

In Situ Hybridization

Dock5-specific mRNA probes were generated by Boster (Hubei, China), and in situ hybridization was performed on cryosections (10 μm in thickness) of wound tissue

according to the manufacturer's instructions. Briefly, after fixation in 4% formaldehyde for 30 min, sections were treated with proteinase in 3% citrate diluent for 5 min at 37°C and prehybridized for 4 h at 40°C. Hybridization with Dock5-specific FITC-labeled mRNA probes was performed overnight at 40°C. Slides were then washed with 2× saline sodium citrate buffer for 15 min to wash away excess probe and hybridization buffers, followed by 0.5× and 0.2× saline sodium citrate buffer at 37°C to remove nonspecific and/or repetitive hybridized DNA/RNA. Probe binding was detected by incubating the sections with streptavidin biotin complex–FITC (1:1,000; Boster) for 1 h at 37°C for superior amplification of the antigen signals. Nuclei were stained with DAPI (Beyotime, Beijing, China) for 5 min at room temperature. The coverslips were mounted with Fluoromount (Boster), and images were acquired by using a fluorescence microscope (cellSens standard 1.15; Olympus, Tokyo, Japan).

Cell Culture and Transfection

Human immortalized keratinocytes (HaCaT cells) were purchased from the Institute of Basic Medical Sciences, Chinese Academy of Medicine Science/Peking Union Medical College (Beijing, China), and were cultured in minimum essential medium/Earle's balanced salt solution medium (HyClone, ThermoFisher, Shanghai, China) with 10% FBS (ExCell, Shanghai, China) in a 5% CO_2 incubator at 37°C. Human epidermal melanocytes and human Langerhans cell–like cell line (ELD-1) were purchased from Chongqing Boer Biotech Co., Ltd., and cultured in DMEM or 1640 medium with 10% FBS. Cell identities were confirmed by the supplier or Shanghai Biowing Applied Biotechnology, Co. (Shanghai, China), and mycoplasma determination was performed by Shanghai Biowing Applied Biotechnology Co. For the knockdown experiment, cells were seeded in six-well plates and transiently transfected with siRNA oligonucleotides at 30 pmol per well using the Lipofectamine RNAiMAX Transfection Reagent (Invitrogen, Waltham, MA) according to the manufacturer's instructions. Dock5-, LAMA3-, ITGA3-, and zinc finger E-box–binding homeobox 1 (ZEB1)–specific and corresponding negative control siRNAs were obtained from Qiagen (Valencia, CA) or RIBOBIO (Guangzhou, China). For overexpression, cells were seeded in six-well plates and transfected with 1 μg plasmid per well using the Lipofectamine 3000 Reagent (Invitrogen) according to the manufacturer's instructions. Dock5 and control vector plasmids were generated by GenScript (Piscataway, NJ).

Confocal Time-Lapse Imaging and Trajectory Analysis

Confluent monolayers of cells were transfected with the siRNA or plasmid of the indicated gene for 24 h, and a scratch wound model then was created. To inhibit cell proliferation, the serum in the medium changed from 10 to 2%. Cells were then placed on the stage of a Leica TCS SP8 microscope (Wetzlar, Germany) in a humidified atmosphere (at 37°C, 5% CO_2) and observed with a 10× lens. Images were acquired every 40 min and analyzed using ImageJ software (National Institutes of Health). Trajectory analysis was performed using the Chemotaxis and Migration Tool 2.0 (Ibidi, GmbH, München, Germany).

Cell Proliferation and Adhesion Assays

For cell proliferation and adhesion assays, HaCaT cells (1×10^3 cells per well for proliferation and 1×10^5 cells per well for adhesion) were seeded into 96-well plates and transfected with the siRNA or plasmid of the indicated gene for 24 h. Cell proliferation was assessed on days 1, 2, and 3. At each time point, 10 μL Cell Counting Kit 8 solution (Dojindo Molecular Technologies, Rockville, MD) mixed with 100 μL fresh culture medium was added to each well and incubated in a 5% CO_2 incubator at 37°C for 40 min. The cell growth curves were acquired by reading the absorbance at 450 nm in the Varioskan Flash Microplate Reader (Thermo Scientific). To study the cell adhesion, cells were placed into two microplates and allowed to attach to the substrates undisturbed in a 5% CO_2 incubator at 37°C for 4 h. At the end of incubation, one of the plates was centrifuged to pellet the cells, and the culture medium was removed; the total cell number was then determined using this plate. In another plate, medium was removed without centrifuge, and the wells were washed with prewarmed (37°C) PBS to remove unattached cells; the number of adherent cells was then determined using this plate. Cell numbers were quantitated using the CyQUANT Cell Proliferation Assay Kit (Invitrogen, Carlsbad, CA) according to the manufacturer's instruction.

Hematoxylin-Eosin, Masson Trichrome, and Immunofluorescence Analyses

Hematoxylin-eosin, Masson trichrome, and immunofluorescence staining were performed on paraffin sections (5 μm in thickness) of skin tissue according to our previous protocols (17). Images were taken using a fluorescence microscope (cellSens standard 1.15; Olympus). The wound widths (distances between wound border hair follicles) and reepithelialization (length of newly formed wound epithelium) were measured using ImageJ (National Institutes of Health). The percentage of proliferating cell nuclear antigen–positive ($PCNA^+$) cells in epithelial tissue was determined by calculating the number of $PCNA^+$ cells divided by the total number (DAPI) of cells. For immunofluorescence staining, the following primary antibodies were used: anti-Dock5 from Novus (Centennial, CO); anti-CK14, anti-CK5, and antivimentin from Santa Cruz Biotechnology (Dallas, TX); anti-CK1, anti-CK10, and anti-Ly6G from Abcam (Cambridge, MA); and anti-CD68 from Proteintech (Hubei, China).

Western Blot, Ubiquitination, and Half-Life Assays

Extraction of skin tissue and cellular protein and Western blot were performed as in our previous protocols (15,16). The following antibodies were used: anti-Dock5 from Novus; anti-Dock1, 3, and 8 and anti-ZEB1 from Proteintech; anti-PCNA (PC10), antivimentin (V9), anti-GAPDH (V-18), and anti-ITGA3 from Santa Cruz Biotechnology; and anti-LAMA3, anti-αSMA, antifibronectin, and anti––collagen I from Abcam. Ubiquitination and half-life assays were performed as described in our previous study (16). Briefly, for the ubiquitination assay, cells were transfected by Dock5 plasmids with hemagglutinin-ubiquitin for 24 h and treated with MG-132 (10 μmol/L) (MCE, Shanghai, China) for 4 h. Cells were harvested, and the lysates were incubated with anti-ZEB1 antibody at 4°C overnight. Ubiquitylated ZEB1 proteins were analyzed by immunoblotting with an antibody against the hemagglutinin epitope. For ZEB1 protein half-life analysis, cells were treated with Dock5 plasmid, and cycloheximide (25 μmol/L) (MCE) was added to block protein synthesis. Cell lysates were collected at the indicated time points after cycloheximide administration and subjected to immunoblot analysis with indicated antibodies.

RNA Sequencing Analysis

The total RNA of wound skin samples from Dock5 KO and WT mice was harvested with Trizol (Takara) and quantified using NanoDrop2000. RNA integrity and genomic DNA contamination were tested by denaturing agarose gel electrophoresis, and the sequencing library was tested using the Agilent 2100 Bioanalyzer with the Agilent DNA 1000 Chip Kit (Agilent Technologies, Waldbronn, Germany). RNA sequencing (RNA-seq) was performed by KangChen Biotech (Shanghai, China) using the Illumina HiSEq 4000 platform.

Streptozotocin-Induced Diabetic Mouse Model

Diabetes was induced in C57BL/6 mice as described in our previous study (17). Briefly, 10-week-old male mice were administered 50 mg/kg streptozotocin (STZ) (dissolved in sodium citrate, i.p. injection; Sigma-Aldrich, St. Louis, MO) for 5 consecutive days. Two weeks after STZ injection, mice with fasting glucose levels >250 mg/dL (13.9 mmol/L) were considered diabetic.

Adenoviruses Mediate Gene Expression or Knockdown in Wounded Mouse Skin

To assess whether LAMA3 mediated the wound healing regulated by Dock5, purified Dock5-expressing (Ade-Dock5) and LAMA3 knockdown adenoviruses and corresponding controls were generated by GENECHEM (Shanghai, China). On the dorsal skin of 8-week-old C57BL/6J mice, 6-mm wound edges were marked, and 2×10^9 plaque-forming units Ade-Dock5 and LAMA3 knockdown adenovirus or their control viruses were injected around each wound. Three days later, 6-mm wounds were created at the marked areas. To evaluate whether Dock5 activation could rescue defective wound healing in STZ mice, 2×10^9 plaque-forming units Ade-Dock5 or control virus were injected around each wound 3 days before wound creation in STZ mice. Wound closure rates were evaluated as described above, and tissues were collected on the indicated day after wounding and processed for analysis.

Primary Keratinocyte Isolation

Primary keratinocytes were isolated from adult mouse epidermises as described before (18). In brief, after mice were euthanized, target skin areas were removed using scissors and placed in a culture dish with epidermis side down. Hypodermises were carefully scraped off using a scalpel blade. The skins were then cut into 1-cm wide strips using scissors and placed with dermis side down in a dish with precooled 0.25% trypsin (Gibco, ThermoFisher) overnight at 4°C. The next day, the epidermis was isolated from the dermis, and keratinocytes were peeled off using the rounded edge of curved forceps for additional mRNA and protein isolations.

Human Skin Tissues

A total of six DFU patients and six healthy participants were recruited after agreeing and providing informed consent. The experimental protocols were approved by the Ethics Committee of the Second Affiliated Hospital of Army Medical University and were consistent with the Declaration of Helsinki.

Statistical Analyses

All data are presented as means ± SEMs unless otherwise indicated. Statistical analysis was performed using GraphPad Prism software (version 7.0) (San Diego, CA). Statistical differences between groups were analyzed using the two-tailed Student *t* test or one-way ANOVA followed by Tukey post hoc test. Both in vitro and in vivo wound closure rates over time were analyzed using two-way ANOVA. A P value <0.05 was considered significant.

Data and Resource Availability

All data related to our conclusions in this report are presented in the main text and/or supplementary materials. Additional data related to this article are available from the corresponding authors upon reasonable request.

RESULTS

Characterization of Dock5 During Skin Wound Healing

We first evaluated the Dock5 expression pattern throughout the entire healing process. Full-thickness 6-mm punch biopsy wounds were made in the dorsal skin of C57BL/6 mice, and skin wound samples after injury (days 0, 1, 3, 5, 7 and 11) were harvested. Our results showed that there was no obvious change in Dock5 expression in the inflammatory phase (1 day), but we confirmed a significant upregulation of Dock5 expression in the wounds

through the proliferative phase (days 3–11) compared with days 0 and 1, although there was a decreased trend after day 5 (Fig. 1*A*). Simultaneously, the other 10 Dock members were examined accordingly. As shown in Supplementary Fig. 1*A*, the relative expression levels of Dock2, 4, 6, 7, 9, 10, and 11 were not significantly changed, whereas along with those of Dock5, the mRNA levels of Dock1, 3, and 8 were significantly increased during wound healing but with different temporal patterns. Dock1 and 8 expression peaked by day 11, and Dock3 expression was highest at day 1. These patterns were further confirmed by the protein expression of Dock1, 3, 5, and 8 (Supplementary Fig. 1*B*). To reveal which cell types were primarily responsible for the changes in Dock5 expression levels during wound healing, we performed in situ hybridization with a Dock5-specific locked oligonucleotide probe on the harvested skin wound sections. The Dock5 signal was mainly detected in epidermal keratinocytes (Fig. 1*B*). In accordance with our mRNA data, Dock5 expression was low in the wounds from day 0 and 1 but gradually increased at day 3, reached its peak at day 5, and subsequently diminished until day 11 after wounding. In addition, we stained Dock5 with different keratinocyte markers and confirmed the colocalization of Dock5 with cytokeratin 14 (Fig. 1*C* and Supplementary Fig. 2). Taken together, these results demonstrate that

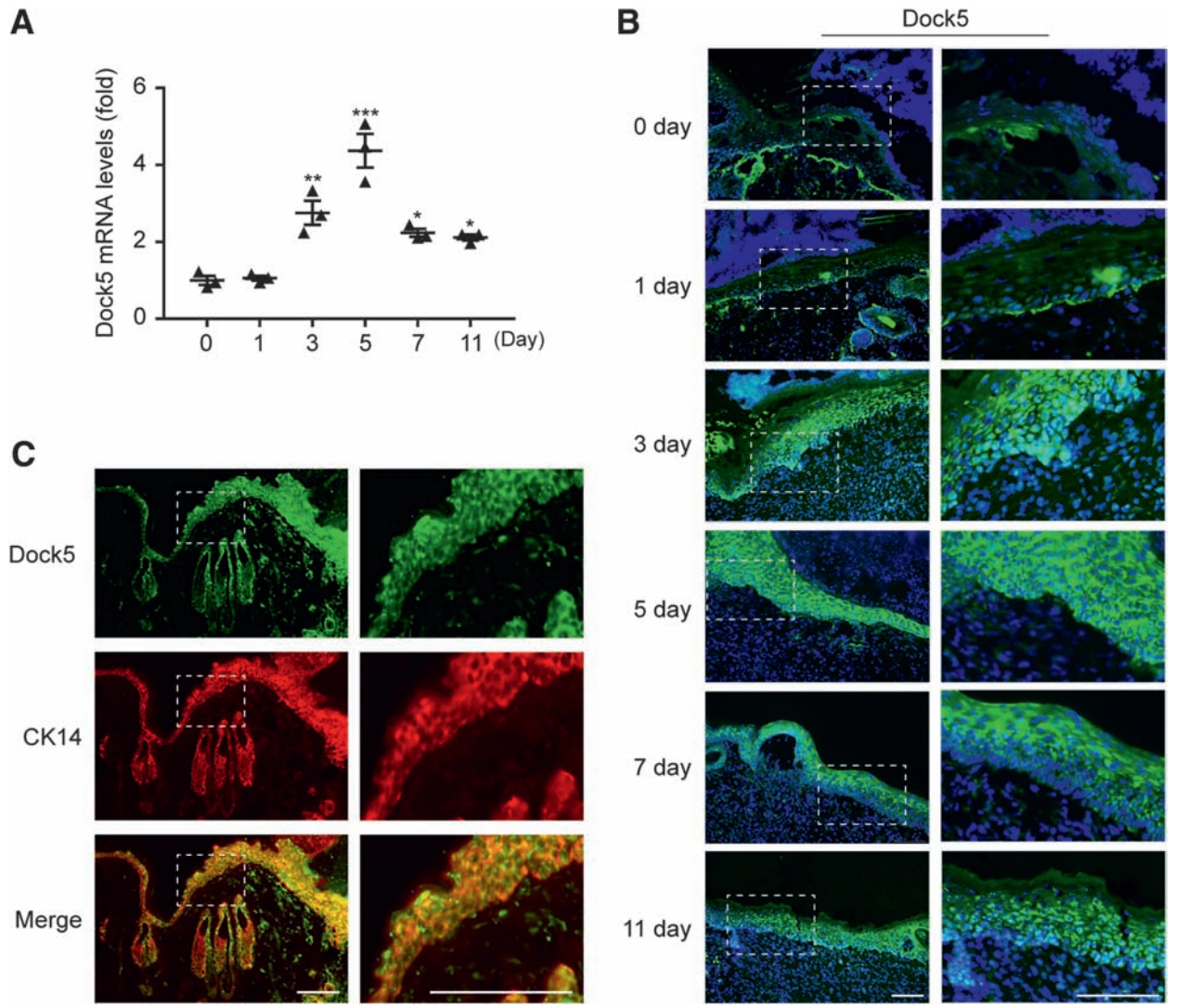

Figure 1—Expression pattern of Dock5 in wounds. Full-thickness wounds were made on the dorsum of C57BL/6 mice. *A*: mRNA expression of Dock5 in wound biopsies at the indicated time points after injury was analyzed by quantitative real-time PCR. *B*: In situ hybridization was performed using a Dock5-specific probe. Green indicates Dock5 expression, and blue indicates DAPI. *C*: Wound sections from C57BL/6 mice were stained for Dock5 (green) and cytokeratin 14 (CK14) (red, keratinocyte marker). Dotted lines in *B* and *C* indicate magnified area. Scale bars, 100 μm for *B* and *C*. $n = 3$ mice per group for *A*–*C*. Data are presented as means ± SEMs. $^{*}P < 0.05$, $^{**}P < 0.01$, $^{***}P < 0.001$.

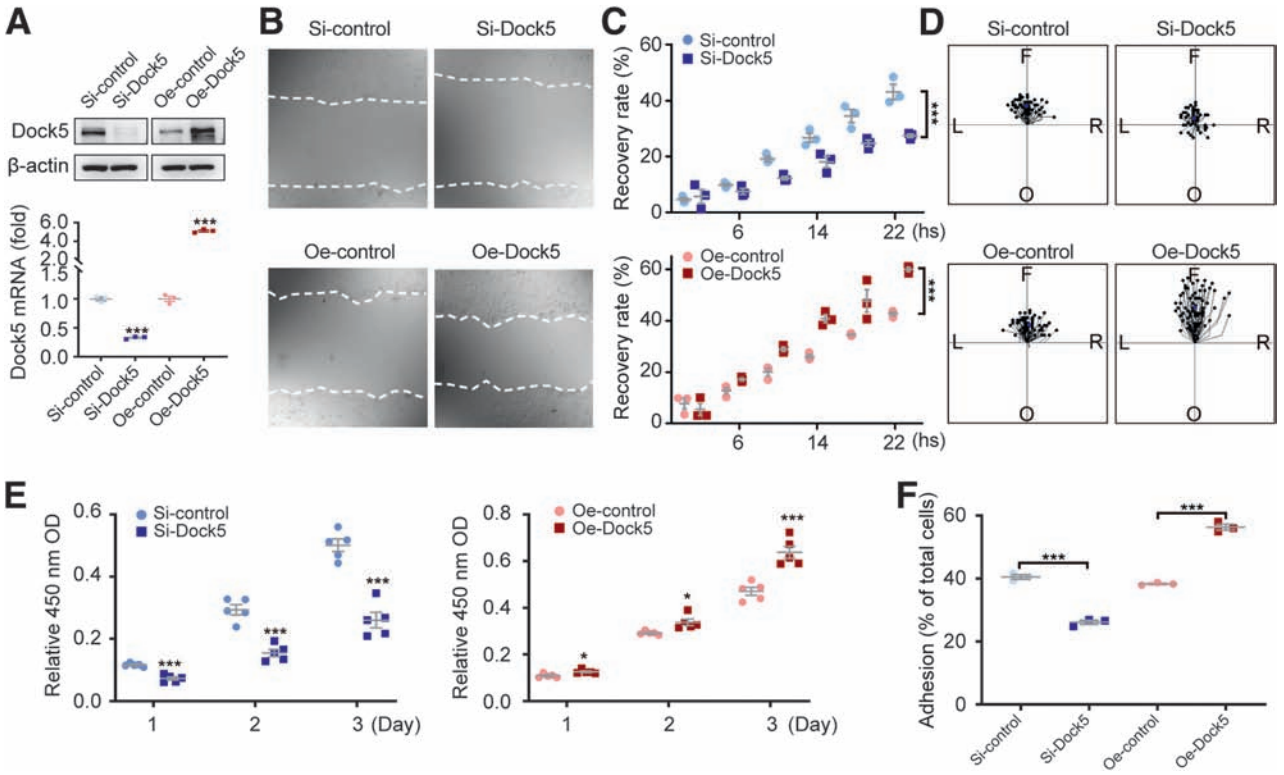

Figure 2—Dock5 regulates keratinocyte migration, proliferation, and adhesion. Keratinocytes were transfected with Dock5-specific siRNA (Si-Dock5) or overexpression plasmid (Oe-Dock5). *A*: The transfection efficiency of overexpression and knockdown is presented. *B*: Live cell images were acquired 16 h after scratching in a wound-healing assay via a live cell imaging system. *C*: Wound recovery rate was quantified. *D*: Cell migration trajectory was tracked for 2 h at 8–10 h after scratching. The center indicates the start point, and magenta dots indicate end points. Each line shows the trajectory of a randomly chosen cell (left [L], right [R], forward [F], or opposite [O] of the direction of migration). *E*: Cell proliferation was assessed by Cell Counting Kit 8 assay. *F*: Cell adhesion was quantified using the CyQUANT Assay Kit. $n = 3$ for *A*–*C* and *F*, $n = 65$–75 for *D*, and $n = 5$ mice per group for *E*. Data are presented as means ± SEMs. $^{*}P < 0.05$, $^{***}P < 0.001$. OD, optical density.

Dock5 expression levels are tightly regulated in epidermal keratinocytes at the wound edge and increase during the proliferation phase.

Dock5 Regulates Various Physiologic Functions in Keratinocytes

To explore the possible role of epidermal Dock5 during the proliferative phase of the wound healing process, we first examined the physiologic functions of migration and proliferation in HaCaT keratinocytes by Dock5 inhibition (si-Dock5) or overexpression (Oe-Dock5) (Fig. 2*A*). As shown in Fig. 2*B* and *C*, significantly delayed migration was observed in the si-Dock5 group compared with the control group, and strikingly accelerated wound closure accompanied overexpression. Cell tracking analyses revealed that, compared with the control cells, most Dock5 knockdown cells showed little or no movement, whereas the Oe-Dock5 group exhibited robust and well-polarized movement during the same time interval (Fig. 2*D*). The proliferation rate of HaCaT cells was then analyzed using the Cell Counting Kit 8 assay, and keratinocyte proliferation was inhibited by silencing Dock5 and enhanced by its overexpression (Fig. 2*E*). We further detected a role of Dock5 in cell adhesion; the dynamics of keratinocytes adhering to the BM could perturb migration and proliferation (4). Keratinocytes with Dock5 knockdown showed a significantly decreased adhesion ability, whereas Oe-Dock5 led to more cells adhering to the uncoated plate surface (Fig. 2*F*), which indicated that Dock5 influenced adhesion, and this effect might have been independent of the exogenous matrix. These data suggest that Dock5 plays an important role in regulating keratinocyte adhesion, migration, and proliferation.

Deficiency of Dock5 Impairs Wound Healing

To investigate whether in vivo Dock5 gene ablation affects skin wound healing, WT and Dock5 KO mice were used (Supplementary Fig. 3*A*). The wound closure rate was assessed via measurement of the wound areas at the indicated time points (Fig. 3*A*). Despite similar blood glucose levels (Fig. 3*B*), Dock5 KO mice exhibited a significantly delayed wound closure rate compared with WT mice (Fig. 3*C*). Reepithelialization (measured by length of neoepithelium) is essential in a

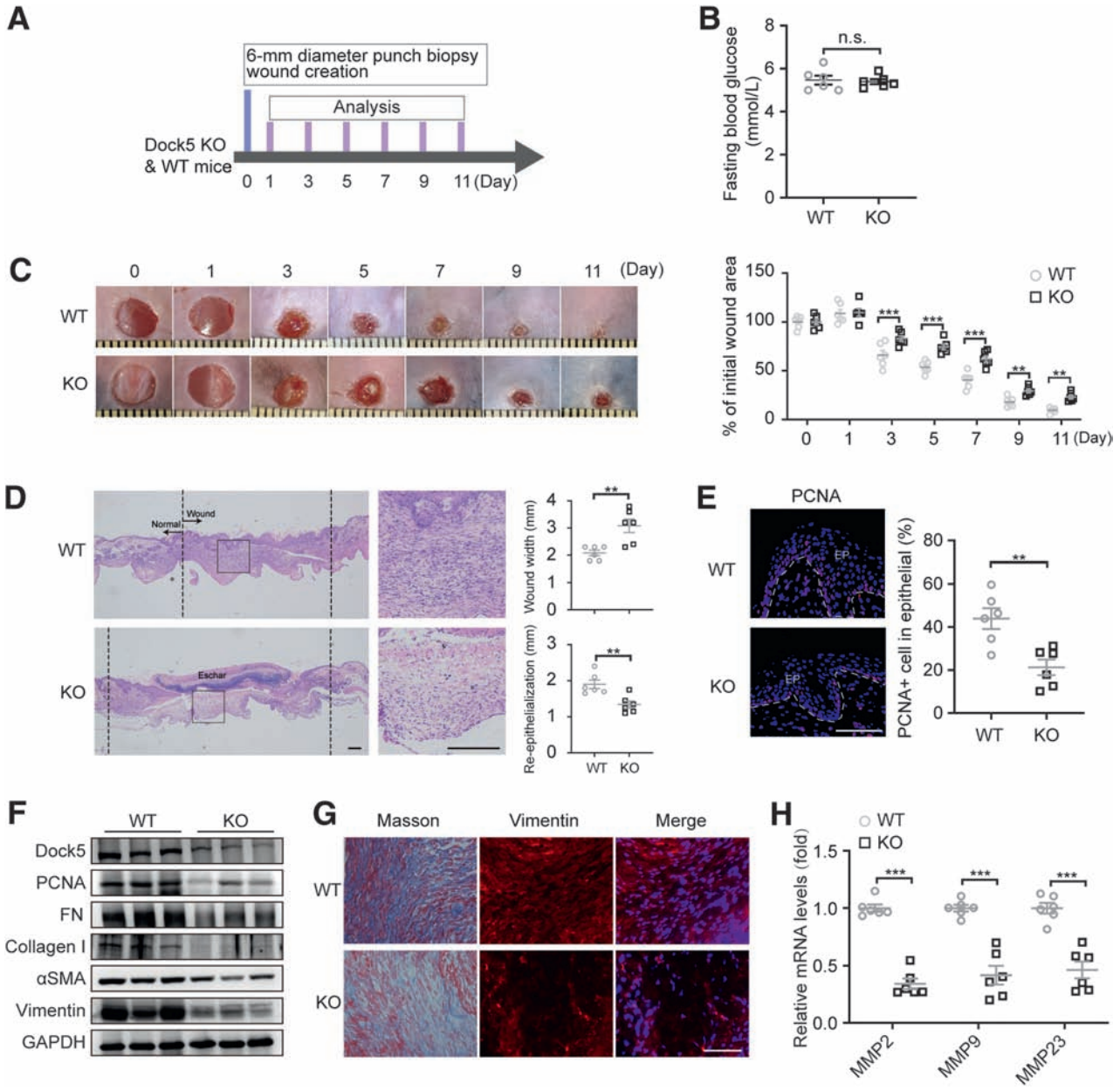

Figure 3—Dock5 KO impedes wound healing. Full-thickness wounds were made on the dorsum of Dock5 KO and WT mice. *A*: Experiment setup. *B*: Fasting blood glucose was assessed. *C*: Representative wound images (left) are shown at the indicated times and were quantified as the percentages of the initial wound area (right). *D*: Representative hematoxylin-eosin–stained sections are shown on day 7 after injury, and wound width and reepithelialization were quantified in WT and KO mice. *E*: The representative images and quantification of $PCNA^+$ cell numbers in epithelial cells are shown. Epithelium (EP) is tagged with dotted lines. *F*: Expression of the indicated proteins in wound tissue from WT and KO mice by Western blot analysis. *G*: Masson trichrome staining and vimentin immunostaining of wound sections from WT and KO mice. *H*: mRNA expression of genes related to ECM deposition was analyzed by quantitative real-time PCR. Each grid scale represents 1 mm for *C*. Scale bars, 200 μm for *D* and 50 μm for *E* and *G*. $n = 6$ mice per group for *A*–*H*. Data are presented as means ± SEMs. $^{**}P < 0.01$, $^{***}P < 0.001$. FN, fibronectin; n.s., not significant.

healed wound to restore an intact epidermal barrier. Morphometric analyses showed that the wound widths were larger and neoepithelial lengths shorter in Dock5 KO healing skin compared with WT at day 7 after injury, indicating defective reepithelialization (Fig. 3*D*). As expected, decreased proliferation, as demonstrated by nuclear $PCNA^+$ cell immunostaining and protein expression, was observed in the Dock5-ablated skin at day 5 after injury (Fig. 3*E* and *F*).

In concert with reepithelialization, collagen is deposited, and matrix proteins form granulation tissue, which serves as the scaffold for keratinocyte migration to replace the previous fibrin clot. The decreased protein levels of matrix fibronectin and collagen I, as well as the

granulation tissue markers αSMA and vimentin, were found in Dock5-deleted skin compared with WT (Fig. 3*F*), which was further confirmed by Masson trichrome and vimentin staining (Fig. 3*G*). Dock5 deficiency also repressed the genes encoding matrix metalloproteinases, which are required for ECM remodeling (1) (Fig. 3*H*). These results indicate that Dock5 KO not only blunts reepithelialization but also suppresses ECM remodeling and granulation tissue formation, which may contribute to the impaired wound healing seen in Dock5 KO skin.

The inflammatory response is an important player in the regulation of wound healing, which begins immediately after wounding via the infiltration of neutrophils and macrophages (1). Neutrophils initiate debridement of devitalized tissues and combat invading microbes and are later removed by macrophages in situ within days (19). However, animal models have shown that an excessive inflammatory response in wound sites impairs keratinocyte migration and proliferation (20,21). Our results showed that Dock5 deficiency in wound tissues did not significantly change mRNA expression of neutrophil chemokines (CXCL1 and CXCL5), macrophage gene MCP-1, or inflammatory cytokines (interleukin-1β [IL-1β], IL-6, and tumor necrosis factor-α) on day 5 of the proliferative phase after injury (Supplementary Fig. 3*B*), which was consistent with the lack of obvious differences detected in the immunofluorescence staining of neutrophils and macrophages using anti-Ly6G and CD68 antibodies, respectively (Supplementary Fig. 3*C*). We also examined the influence of Dock5 inactivation during inflammatory states. Results shown in Supplementary Fig. 3*D* and *E* were in agreement with no apparent differences in wound closure between Dock5 KO and WT mice 1 day after injury (Fig. 3*C*). However, we observed a relatively increased trend of cytokine gene expression in Dock5 KO skin, although this expression was not statistically significant, except for IL-6 (Supplementary Fig. 3*D*).

Next, we wanted to assess whether the delayed wound healing of Dock5 KO mice was due to the abrogation of Dock5 in keratinocytes. We used a conditional KO mouse model in which Dock5 was specifically ablated in keratinocytes by crossing $Dock5^{flox/flox}$ mice with keratin14-Cre mice (14,22). After wounding, these mice presented an impaired healing phenotype similar to the Dock5 KO mice (Fig. 3), which was evidenced as delayed reepithelialization and suppressed ECM remodeling and granulation compared with Cre^{+} $Dock5^{WT/WT}$ mice (controls) (Supplementary Fig. 4*A–H*). These results indicate that Dock5 deficiency in keratinocytes may be the major contributor to the impairment of wound healing observed in Dock5 KO skin. There are several surrounding immune/structural cells in addition to keratinocytes in the epidermis, such as Langerhans cells and melanocytes (23). Previous studies have reported that epidermis-resident Langerhans cells release a rapid pulse of chemokines and cytokines in early acute inflammation (24), and enhanced proliferation and migration of melanocyte also favor the regeneration of an intact differentiated and pigmented epidermis to restore the outermost skin barrier (25). Therefore, we assessed whether Dock5 influenced the physiologic functions of these two cells. Our results showed that neither si-Dock5 nor Oe-Dock5 significantly influenced melanocyte migration or proliferation (Supplementary Fig. 4*I–L*), but the cytokines transforming growth factor-β and IL-23 were increased in lipopolysaccharide-stimulated Langerhans cells with Dock5 knockdown (Supplementary Fig. 4*M*). These results suggest that Dock5 mediates the function of Langerhans cells, which may also be involved in the healing process in wounds.

Dock5 Regulates Laminin-332/Integrin Signaling During Wound Healing

To gain insight into the molecular mechanism behind the participation of Dock5 in wound healing, we used an unbiased method (i.e., RNA-seq analysis). Comparison of the Dock5 KO and WT groups identified a total of 702 significantly changed and differentially expressed genes (105 upregulated and 597 downregulated genes; $\log_2$FC >1.5) (Supplementary Table 2). Hierarchic clustering of differentially expressed genes showed distinct patterns between these two groups (Fig. 4*A*). Further biologic function analysis showed that gene ontology terms associated with signal transduction and cellular process, such as regulation of cell proliferation and migration, were obviously changed (Fig. 4*B* and Supplementary Table 3). Kyoto Encyclopedia of Genes and Genome (KEGG) analysis showed the 10 most enriched pathways for the genes downregulated and upregulated by Dock5 (Fig. 4*C*, Supplementary Fig. 2, and Supplementary Table 4). Intriguingly, consistent with our hypothesis that keratinocyte Dock5 plays a vital role in cutaneous wounds, many of the annotated genes from the significantly downregulated gene list ($P < 0.01$) coded for proteins important in responding to epidermal cell functions (e.g., Casp14, Myh9, Adam17, and Hdac1) (26–29). In particular, pathways termed focal adhesion and ECM-receptor interaction were noted in the top three for downregulated gene enrichment.

To maintain epidermal integrity, intracellular signals are transduced by keratinocytes interacting with ECM proteins, which occurs mainly through laminin binding to its receptor integrin (5,6). Laminin-332 (previously known as laminin-5), trimerized by α3, β3, and γ2 chains, is a secreted ECM protein and major adhesive ligand of the epidermal BM. Laminin-332 specifically incorporates two integrin receptors, Itgα3β1 and Itgα6β4, both of which are also highly conserved in epidermal keratinocytes (5,30), to induce cellular activities such as adhesion, migration, and proliferation. Therefore, we speculated that laminin-332/integrin signaling was involved in Dock5-modulated wound healing. Our results showed that genes encoding three laminin-332 chains (LAMA3, LAMB3, and LAMC2) and two integrin subunits (ITGA3 and ITGB4) exhibited significant changes in the

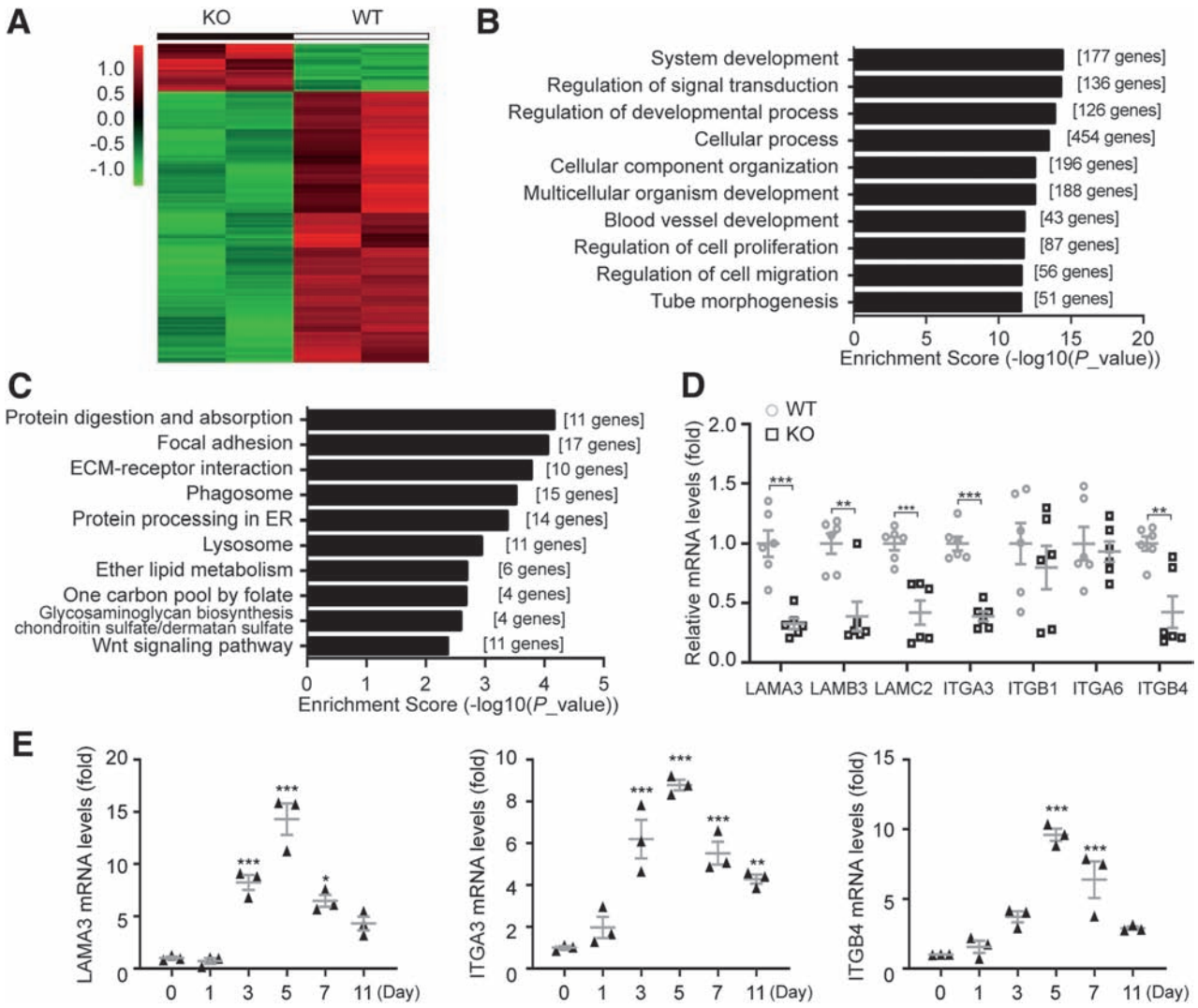

Figure 4—Dock5 regulates laminin-332/integrin signaling during wound healing. *A*: Hierarchic clustering of all significantly differentially expressed genes in wound tissue at day 5 after injury. *B*: Gene ontology analysis of all significantly altered genes was performed, and the top 10 items are shown. *C*: KEGG pathway analysis was conducted on all significantly downregulated genes, and the top 10 items are shown. *D*: Gene expression of all three chains of laminin-332 and its two integrin receptors in wound tissue from WT and KO mice was assessed by quantitative real-time PCR (qRT-PCR). *E*: mRNA expression of indicated genes in wound biopsies at the indicated time points after injury was analyzed by qRT-PCR. $n = 6$ mice per group for *D*, and $n = 3$ for *E*. Data are presented as means ± SEMs. $^*P < 0.05$, $^{**}P < 0.01$, $^{***}P < 0.001$. ER, endoplasmic reticulum.

comparison between WT and KO repaired skin tissue (Fig. 4*D*). Moreover, LAMA3, ITGA3, and ITGB4 presented augmented expression similar to the dynamic pattern of Dock5 seen in Fig. 1*A* during the course of wound healing (Fig. 4*E*), indicating that they may have a close association. Because there is ample evidence of the physiologic importance of laminin-332 interaction with these integrins in epidermal cell motility and healing (31,32), we then investigated the role of laminin-332 in Dock5-regulated skin repair.

Dock5 Improves Wound Healing by LAMA3 Activation Through Promoting ZEB1 Ubiquitination

Because the α chain of laminin-332 is essential for binding with Itgα3β1 and Itgα6β4 (33,34), the effects of laminin α3 deficiency under Dock5-controlled wound healing were then evaluated (Fig. 5*A*). Indeed, compared with the control group, the wound closure rate was accelerated in mice with Dock5 intradermal administration to delivery to the epidermal layer (35) (Fig. 5*B* and *C*). Knocking down the α chain of laminin-332 (adenovirus-sh-LAMA3) at wound edges substantially attenuated the wound closure rate, reepithelialization, collagen deposition, and granulation seen in Dock5-overexpressing mice (Fig. 5*B*–*E*). The in vitro data further confirmed that LAMA3 siRNA significantly abolished the enhanced cell adhesion, migration, and proliferation by Dock5 transient transfection (Supplementary Fig. 3*A*–*E*), indicating that Dock5 improved wound healing via LAMA3 activation. In

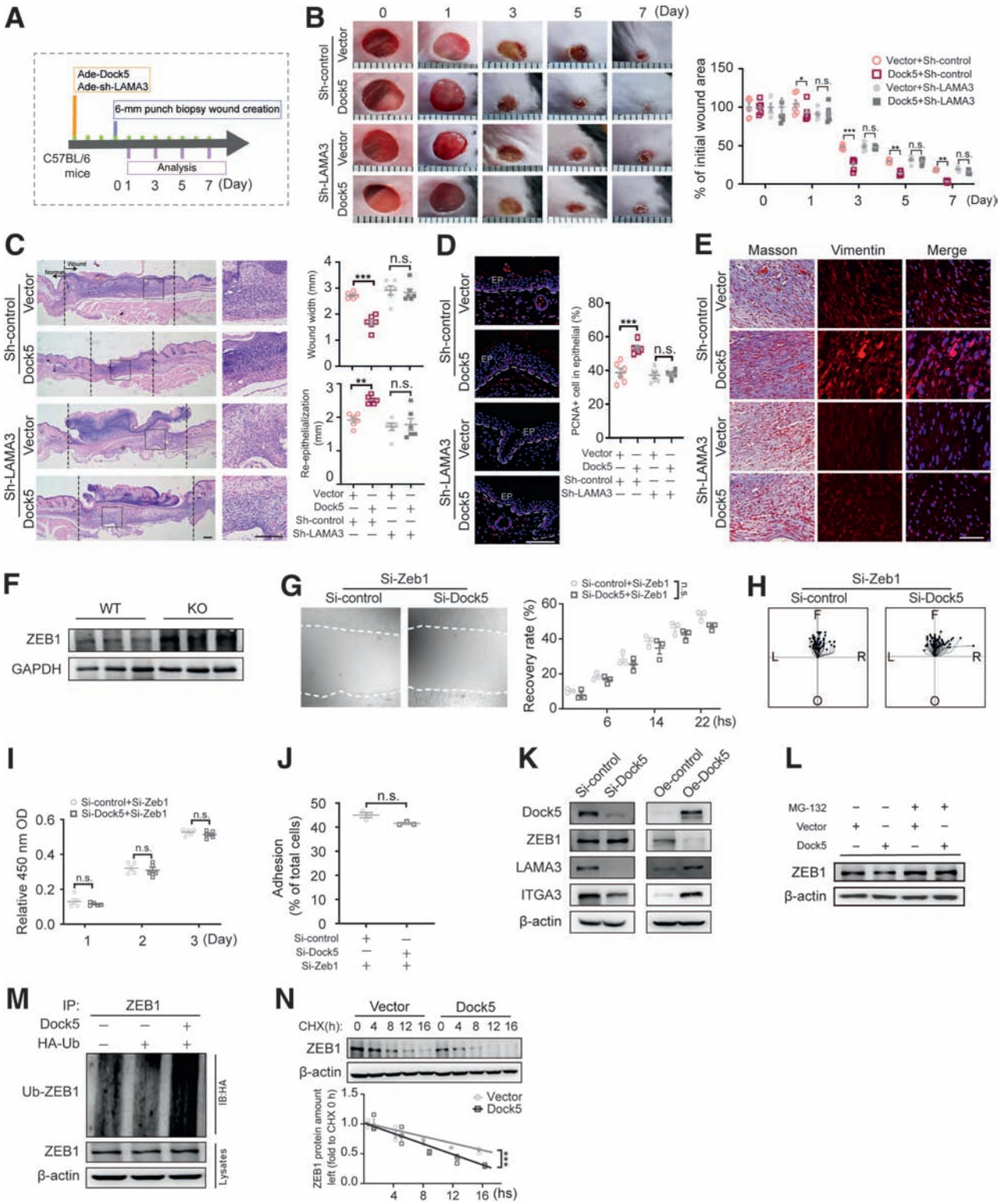

Figure 5—Dock5 accelerates wound healing by LAMA3 activation through promoting ZEB1 ubiquitination. *A*: Schematic representation of the experiment setup used for evaluating whether Dock5-regulated wound healing occurs through LAMA3. Dock5-expressing and LAMA3 knockdown adenoviruses (Ade) were intradermally injected around the wound areas 3 days before the full-thickness wounds were made in C57BL/6 mice. *B*: Representative wound images (left) are shown at the indicated times and quantified as the percentages of the initial wound area (right). *C*: Representative hematoxylin-eosin–stained sections (left) are shown on day 7 after injury, and wound width and reepithelialization (right) were quantified. *D*: The representative images and quantification of $PCNA^+$ cell numbers in epithelial cells are shown. Epithelium (EP) is tagged with dotted lines. *E*: Masson trichrome staining and vimentin immunostaining of wound sections from indicated mice. *F*: Expression of the ZEB1 proteins in wound tissue from WT and KO mice by Western blot analysis. Keratinocytes were transfected with Zeb1-specific siRNA with or without Dock5-specific siRNA. *G*: Live cell images (left) were acquired 16 h after

addition, the manipulation of ITGA3, the laminin-332 receptor, could also interfere with Dock5-medicated physiologic functions in epidermal keratinocytes (Supplementary Fig. 4*A–E*). Taken together, Dock5 improved cell behaviors for repairing skin tissue in a LAMA3-dependent manner.

Next, we explored the regulation of Dock5 on LAMA3. A previous study suggested that a dual zinc finger homeodomain transcription factor, ZEB1, could directly regulate the mRNA expression of all three chains of laminin-332 (36), which was consistent with our observations of the skin of Dock5 KO mice. Moreover, ZEB1 deletion was recently reported to promote directional migration and proliferation of skin epithelial cells (37). Therefore, we investigated the participation of ZEB1 in Dock5-regulated downstream effects. The skin of Dock5-deficient mice presented augmented ZEB1 protein expression (Fig. 5*F*). Furthermore, ZEB1 siRNA abrogated the suppressed cell motility caused by Dock5 knockdown in HaCaT cells (Fig. 5*G–J*), suggesting that the Dock5-mediated effects occurred through ZEB1 inhibition.

To question the molecular mechanism underlying how Dock5 regulates ZEB1, we examined ZEB1 expression, along with LAMA3 and ITGA3 under Dock5 manipulation. In HaCaT cells, the protein expression of LAMA3 and ITGA3 was enhanced with Dock5 overexpression and attenuated by Dock5 siRNA (Fig. 5*K*), which was consistent with our in vivo data (Fig. 4*D*). Our results also showed that ZEB1 protein, but not mRNA, levels were altered by Dock5 loss- and gain-of-function modulation (Fig. 5*K* and Supplementary Fig. 5), indicating a posttranscriptional mechanism. In addition, ZEB1 protein was negatively regulated by Dock5, and a previous study showed that ZEB1 could be modulated through its degradation by the proteasomal pathway (38); we then assessed this pathway. The proteasome inhibitor MG132 blocked the Dock5 overexpression–induced reduction in ZEB1 protein (Fig. 5*L*). Moreover, Dock5 overexpression increased ubiquitination (Fig. 5*M*) and decreased the half-life of the ZEB1 protein (Fig. 5*N*). These results indicated that Dock5 regulated the stabilization of the ZEB1 protein via the proteasomal degradation pathway.

Rescue of Dock5 Accelerates Wound Healing in Diabetic Mice

On the basis of the observed effects of Dock5 mediation of reepithelialization, ECM deposition, and granulation in the skin wound, we then explored its role under pathologic conditions. Our results showed lower Dock5 expression in the epidermal skin of DFU patients compared with healthy participants (Fig. 6*A* and Supplementary Table 5). These results were replicated in mouse models of type 1 diabetes (STZ-induced diabetic mice) and type 2 diabetes (db/db mice) at both the mRNA and protein levels (Fig. 6*B*). After finding this downregulation of Dock5, we next determined the effects of rescuing Dock5 expression on wound healing during diabetes. The restoration of Dock5 and the accompanying decrease in ZEB1 were confirmed in isolated keratinocytes from skin tissues in overexpression studies (Fig. 6*C*). In accordance with previous observations, STZ treatment indeed induced impaired wound healing and retarded reepithelialization, whereas rescue of Dock5 via intradermal adenoviral injection to the STZ wounds blocked delayed healing (Fig. 6*D–F*). Moreover, the increased expression of LAMA3 and ITGA3 and the downstream effects of ECM remodeling and granulation were observed with Dock5 replenishment (Fig. 6*G–I*), corroborating our in vitro mechanistic findings, which further confirmed that these tissues underwent a more efficient healing process. In sum, these findings indicate that rescue of Dock5 promotes diabetic wound healing and may be a promising therapeutic target for DFUs.

DISCUSSION

Patients with diabetes experience impaired wound healing, which may lead to limb amputation or even cause death. The current study identified Dock5 as a critical regulator of cutaneous wound healing, and the mechanistic experiments indicated that the effects occurred mainly through ZEB1-controlled LAMA3/ITGA3 signaling. Moreover, in patients and animal models of diabetes, Dock5 expression at the skin edge was reduced, and rescuing Dock5 expression led to a significant improvement in cutaneous wound repair.

Our findings suggest that Dock5 is a critical regulator of skin wound closure by stimulating laminin-332 to facilitate integrin-mediated adhesion, migration, and proliferation of keratinocytes, resulting in faster tissue regeneration. Sixteen laminin heterotrimers with different combinations of 6α, 3β, and 3γ chains have been

scratching in a wound-healing assay via a live cell imaging system, and the wound recovery rate was quantified (right). *H*: Cell migration trajectories were tracked for 2 h at 8–10 h after scratching. The center indicates the start point, and magenta dots indicate end points. Each line shows the trajectory of a randomly chosen cell (left [L], right [R], forward [F], or opposite [O] of the direction of migration). *I*: Cell proliferation was assessed by Cell Counting Kit 8 assay. *J*: Cell adhesion was quantified using the CyQUANT Assay Kit. *K*: Keratinocytes were transfected with Dock5-specific siRNA or Dock5 overexpression plasmid, and indicated proteins were detected. *L–N*: Keratinocytes were transfected by Dock5 plasmid, and ZEB1 protein was examined 4 h after proteasomal inhibitor MG-132 (10 μmol/L) addition (*L*). Hemagglutinin (HA)-tagged ubiquitin (Ub) was cotransfected with or without Dock5 plasmid, and ubiquitination was detected (*M*). The half-life of ZEB1 protein was determined by pulse-chase assay with protein synthesis inhibitor cycloheximide (CHX) (25 μmol/L) administration (*N*). Each grid scale represents 1 mm for *B*. Scale bars, 200 μm for *C*, and 50 μm for *D* and *E*. $n = 3$ mice per group for *G* and *J–N*, $n = 5$ for *I*, $n = 69–75$ for *H*, $n = 6$ for *A–F*. Data are presented as means ± SEMs. $^*P < 0.05$, $^{**}P < 0.01$, $^{***}P < 0.001$. IB, immunoblotting; IP, immunoprecipitation; n.s., not significant; OD, optical density.

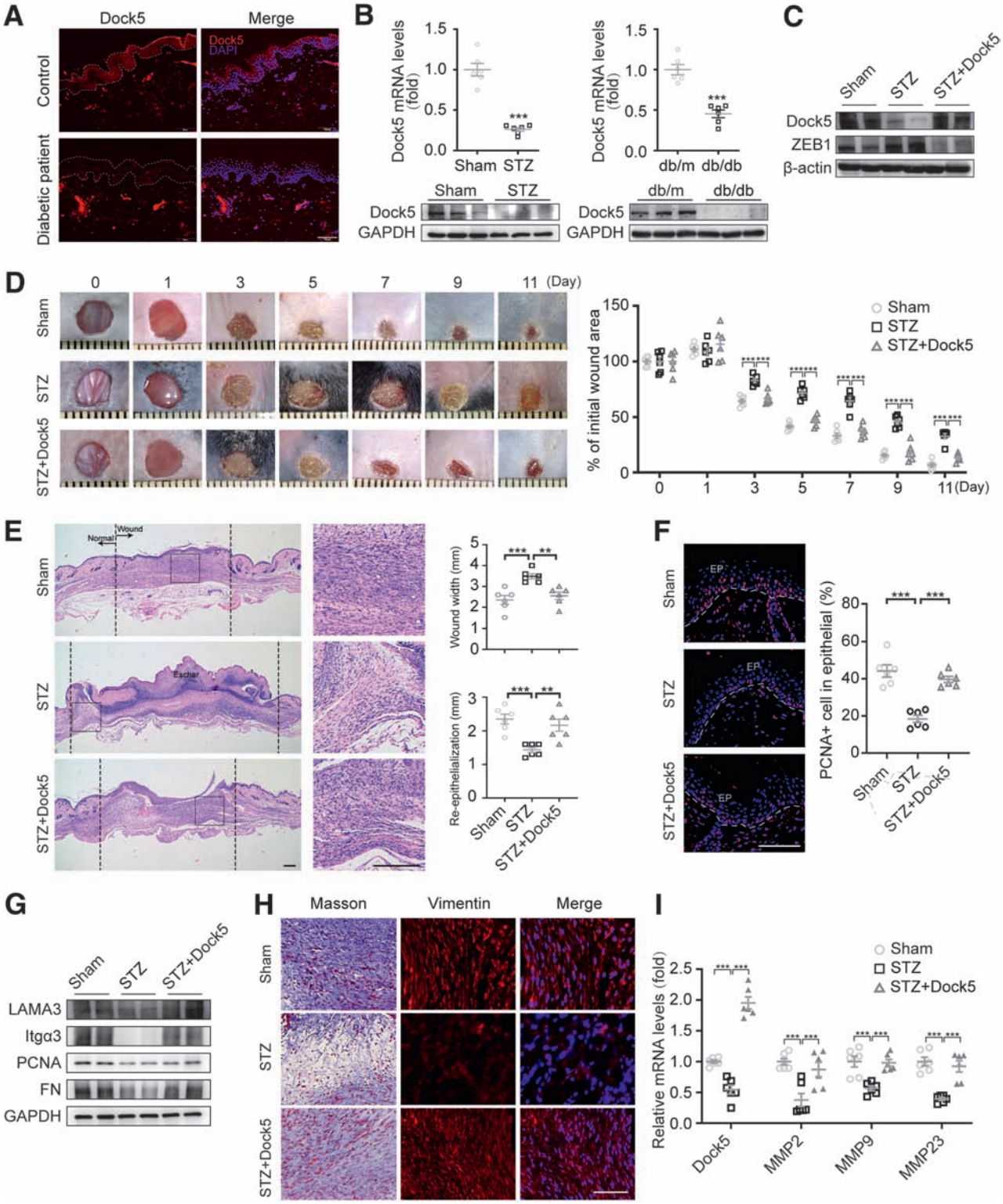

Figure 6—Rescue of Dock5 accelerates wound healing in diabetic mice. *A*: Skin tissue surrounding the wounds of patients with diabetes was sampled and immunostained for Dock5. Epithelium (EP) is tagged with dotted lines. *B*: mRNA and protein levels of Dock5 were analyzed in wound tissue of STZ and db/db mice. Full-thickness wounds were made on the dorsum of control (Sham) and STZ-injected mice, and Dock5-expressing adenovirus was then intradermally injected into each wound of the STZ group mice 3 days before the wounds were created. *C*: The protein expression of Dock5 and ZEB1 was assessed in isolated keratinocytes from wound tissues. *D*: Representative wound images (left) are shown at the indicated times, and healing was quantified as the percentage of the initial wound area (right). *E*: Representative hematoxylin-eosin–stained sections (left) are shown on day 7 after injury, and the wound width and reepithelialization (right) were quantified. *F*: The representative images and quantification of $PCNA^+$ cell numbers in epithelial cells are shown for each group. *G*: Expression of the indicated proteins in wound tissue from mice by Western blot analysis. *H*: Masson trichrome staining and vimentin

demonstrated to exist in vivo (6). The α chain is thought to be the most important, not only in determining the tissue-specific distribution and biologic activity of the laminin isoforms but also in interacting with cell surface receptor integrins through the G domain (33,34). Our results showed that Dock5 was capable of affecting the expression of three chains of laminin-332, and deletion of the α chain, which was derived from the individual LAMA3 gene, abrogated Dock5-promoted wound closure and cellular activities in vivo and in vitro. Similar results could be recapitulated under ITGA3 knockdown circumstances in cultured keratinocytes, suggesting that Dock5 effects are required for laminin-332–binding integrins to proceed, which was supported by a number of laminin-332 or ITGA3 knockdown and functional inhibition studies on keratinocytes in epidermal repair (32,39,40). Moreover, we observed delayed formation of granulation tissue by suppressing ECM production and collagen deposition in the skins of Dock5-null mice; however, its overexpression in the epidermis ameliorated these pathologic features in diabetic mice. These results strengthened the functional reports regarding the impact of laminin-332 and ITGA3 on maintaining homeostasis in multiple organs through crosstalk from epidermal to endothelial cells (41,42), underscoring the importance of Dock5-regulated LAMA3/ITGA3 signaling in tissue morphogenesis. We also observed that the expression of LAMB3 and LAMC2 could be altered by Dock5 manipulation, and additional studies on the participation of these two chains in Dock5-regulated skin are warranted. In addition, a previous study reported that Dock2 and 5 are dispensable in integrin-dependent neutrophil adhesion (43), but we revealed an essential role of Dock5 regulation in keratinocyte activities via ITGA3. Furthermore, in addition to adhesion, migration, and proliferation, the effects of Dock5 on inflammation and macrophage were examined because of the important role of the inflammatory response during wound healing. Although no marked changes were detected during the proliferative phase, Dock5 ablation in skin increased the expression of several cytokine genes, especially IL-6, in the inflammatory status, which requires further investigation of its potential function and regulatory mechanisms. Notably, we used a keratinocyte-specific KO mouse model and confirmed that the retarded healing in Dock5 KO skin was primarily due to its deficiency in keratinocytes. The influence of Dock5 on the surrounding Langerhans cells and melanocytes was also seen in our study, indicating that although keratinocytes account for 95% of all epidermal cells, the expression and functional relevance of Dock5 in the remaining 5%, including melanocytes, Langerhans cells, and Merkel cells, and the few dermal cells shown in Fig. 1 cannot be completely excluded.

We found that Dock5 induced LAMA3 signaling by promoting ZEB1 ubiquitination, which may be an undiscovered mechanism for the distinct cell behaviors mediated by the laminin-332–binding integrin in the cutaneous microenvironment. ZEB1 is considered an epithelial-mesenchymal transition transcriptional activator for tumor cell activities. Recent studies have disclosed that both ZEB1 and another ZEB family member, ZEB2, attenuate keratinocyte adhesion and disrupt collective and directional migration toward the wound center for efficient reepithelialization, leading to compromised integrity of the epidermal barrier (37,44,45). Our results provide further evidence for this concept by showing that suppression of cell adhesion and migration by knocking down Dock5 was blunted by ZEB1 deletion, indicating that Dock5 might be an upstream regulator of ZEB1 during these processes. Moreover, our study suggests that Dock5 regulates ZEB1 degradation through the proteasomal pathway. Because the Siah1/2 E3 ligases and Skp1-Pam-Fbxo45 atypical ubiquitin E3 ligase complex have been shown to promote ZEB1 ubiquitination and degradation during tumor metastasis (46,47), the specific mechanism of Dock5-ZEB1 interplay in the ubiquitin ligase complex favoring ZEB1 degradation in keratinocytes is worthy of exploration, and it may be an efficacious target for therapies aimed at improving wound healing.

During the process of analyzing information from RNA-seq, we focused on KEGG pathways because focal adhesion and ECM-receptor interaction, which were in the top three for downregulated genes, were consistent with the phenotypes observed in Dock5-deficient wounds and keratinocytes; Dock5 was found to be mainly expressed in keratinocytes, and in literature searches, laminin-integrin interaction (6), Notch signaling (48), and mitogen-activated protein kinases (49) were reported to be involved primarily in keratinocyte-mediated focal adhesion and ECM remodeling. We measured these pathways and did not find significant changes in genes of Notch signaling or major members of mitogen-activated protein kinases (data not shown). Genes encoding laminin-332 and its two integrin subunits were markedly decreased in Dock5 KO skin; however, in RNA-seq data, ITGA3 and ITGB4 showed only a decreasing trend without significance, and this inconsistency may have been due to the inclusion of more skin samples from Dock5 KO and WT mice in the quantitative PCR analysis. Our KEGG analysis also showed that some other pathways were also affected by Dock5, such as the downregulation of protein processing in the endoplasmic reticulum and the Wnt signaling

immunostaining of wound sections are shown for the indicated groups. *I*: mRNA expression of genes related to ECM deposition was analyzed by quantitative real-time PCR. Each grid scale represents 1 mm for *D*. Scale bars, 100 μm for *A*, 200 μm for *E*, and 50 μm for *F* and *H*. $n = 6$ patients or mice per group for *A*–*I*. Data are presented as means ± SEMs. $^{**}P < 0.01$, $^{***}P < 0.001$.

pathway. Previous studies have reported several important functions of these pathways in skin wound healing; for example, the endoplasmic reticulum chaperone oxygen-regulated protein 150 in macrophages suggests that a promoter for angiogenesis (50) and Wnt/β-catenin signaling is associated with dermal fibrosis (51). These additional possible effects of Dock5 in cutaneous wound healing will be the subjects of further investigation of Dock5-regulated healing.

Our study provides a potential therapeutic target for skin wound healing impairment during diabetes. Deficient Dock5 expression was identified in the wound edges of patients and animal models of diabetes. Rescuing Dock5 expression substantially promoted wound healing in STZ mice, which indicates the therapeutic potential of targeting Dock5. Our finding is further supported by previous evidence of increased ZEB1 and decreased laminin-332 expression in diabetic cutaneous ulcers, as well as improved wound healing with deletion of ZEB1 or topical laminin-332 application (44,52). Studies by our colleagues and others have suggested that several antidiabetic agents (DPP4 inhibitors, SGLT-2 inhibitors, and GLP-1 agonists) and antioxidants (sulforaphane and cinnamaldehyde) are capable of promoting skin wound repair (15,53–55). Therefore, additional investigations are required to explore the potential relationships between Dock5 and these therapies and their effects on skin wounds.

We observed no change in blood glucose between Dock5 WT and KO mice receiving normal chow, which was in accordance with the recent study on the involvement of Dock5 in hepatic glucose metabolism (12). Deletion of Dock5 in mice receiving a high-fat diet proved to reduce energy expenditure and insulin sensitivity and promote obesity by activating the mTOR/S6K1 pathway. Because mounting evidence also suggests a potential role of Dock5 in metabolic processes (11,56), future studies investigating the impact of Dock5 on other tissues and organs are warranted.

Collectively, our findings reveal a novel role of Dock5 in regulating the function of epithelial cells and skin wound healing. In addition, activation of the Dock5/LAMA3 pathway via destabilizing ZEB1 in skin might be an important mechanism for ameliorating the impairment of wound healing during diabetes based on our in vitro explorations and animal model recapitulations. Direct targeting of Dock5 may also have therapeutic potential.

Funding. This work was supported by grants from the National Science Fund for Distinguished Young Scholars (81925007), National Natural Science Foundation of China (82000769, 82070881, 82070836, 81700714, 81721001, and 81970752), "Talent Project" of the Army Medical University (2017R013, 2019R047, and 2019XQYYYJ003-2), and the Macau Young Scholars Program (AM201918).

Duality of Interest. No potential conflicts of interest relevant to this article were reported.

Author Contributions. H.Q., T.M., Y.W., and L.T. contributed equally to this work. H.Q., T.M., L.T., L.Z., X. Liu, M.L., R.Z., X. Liao, and X.X. were responsible for acquisition of data and statistical analysis. Y.W., B.H., X.G., J.W., and J.Y. were responsible for analysis and interpretation of data. H.Q., T.M., and Y.Z. drafted the manuscript. J.L., X. Li, G.Y., Z.Z., H.Z., and Y.Z. critically revised the manuscript for important intellectual content. H.Z. and Y.Z. are the guarantors of this work and, as such, had full access to all the data in the study and take responsibility for the integrity of the data and the accuracy of the data analysis.

References

1. Eming SA, Martin P, Tomic-Canic M. Wound repair and regeneration: mechanisms, signaling, and translation. Sci Transl Med 2014;6:265sr6
2. Raja, Sivamani K, Garcia MS, Isseroff RR. Wound re-epithelialization: modulating keratinocyte migration in wound healing. Front Biosci 2007;12:2849–2868
3. Simpson CL, Patel DM, Green KJ. Deconstructing the skin: cytoarchitectural determinants of epidermal morphogenesis. Nat Rev Mol Cell Biol 2011;12:565–580
4. Watt FM. Mammalian skin cell biology: at the interface between laboratory and clinic. Science 2014;346:937–940
5. Longmate WM, Dipersio CM. Integrin regulation of epidermal functions in wounds. Adv Wound Care (New Rochelle) 2014;3:229–246
6. Iorio V, Troughton LD, Hamill KJ. Laminins: roles and utility in wound repair. Adv Wound Care (New Rochelle) 2015;4:250–263
7. Boulton AJ, Vileikyte L, Ragnarson-Tennvall G, Apelqvist J. The global burden of diabetic foot disease. Lancet 2005;366:1719–1724
8. Gadea G, Blangy A. Dock-family exchange factors in cell migration and disease. Eur J Cell Biol 2014;93:466–477
9. Laurin M, Fradet N, Blangy A, Hall A, Vuori K, Côté JF. The atypical Rac activator Dock180 (Dock1) regulates myoblast fusion in vivo. Proc Natl Acad Sci U S A 2008;105:15446–15451
10. Vives V, Cres G, Richard C, et al. Pharmacological inhibition of Dock5 prevents osteolysis by affecting osteoclast podosome organization while preserving bone formation. Nat Commun 2015;6:6218
11. Ogawa K, Tanaka Y, Uruno T, et al. DOCK5 functions as a key signaling adaptor that links FcεRI signals to microtubule dynamics during mast cell degranulation. J Exp Med 2014;211:1407–1419
12. Lai Y, Zhao A, Tan M, et al. DOCK5 regulates energy balance and hepatic insulin sensitivity by targeting mTORC1 signaling. EMBO Rep 2020;21:e49473
13. Liu C, Guo T, Xu G, et al. Characterization of alternative splicing events in HPV-negative head and neck squamous cell carcinoma identifies an oncogenic DOCK5 variant. Clin Cancer Res 2018;24:5123–5132
14. Vassar R, Rosenberg M, Ross S, Tyner A, Fuchs E. Tissue-specific and differentiation-specific expression of a human K14 keratin gene in transgenic mice. Proc Natl Acad Sci U S A 1989;86:1563–1567
15. Long M, Cai L, Li W, et al. DPP-4 inhibitors improve diabetic wound healing via direct and indirect promotion of epithelial-mesenchymal transition and reduction of scarring. Diabetes 2018;67:518–531
16. Zheng Y, Qu H, Xiong X, et al. Deficiency of mitochondrial glycerol 3-phosphate dehydrogenase contributes to hepatic steatosis. Hepatology 2019;70:84–97
17. Zheng H, Whitman SA, Wu W, et al. Therapeutic potential of Nrf2 activators in streptozotocin-induced diabetic nephropathy. Diabetes 2011;60:3055–3066
18. Lichti U, Anders J, Yuspa SH. Isolation and short-term culture of primary keratinocytes, hair follicle populations and dermal cells from newborn mice and keratinocytes from adult mice for in vitro analysis and for grafting to immunodeficient mice. Nat Protoc 2008;3:799–810
19. Sun BK, Siprashvili Z, Khavari PA. Advances in skin grafting and treatment of cutaneous wounds. Science 2014;346:941–945

20. Stavrou EX, Fang C, Bane KL, et al. Factor XII and uPAR upregulate neutrophil functions to influence wound healing. J Clin Invest 2018;128:944–959
21. Mori R, Power KT, Wang CM, Martin P, Becker DL. Acute downregulation of connexin43 at wound sites leads to a reduced inflammatory response, enhanced keratinocyte proliferation and wound fibroblast migration. J Cell Sci 2006;119:5193–5203
22. Vasioukhin V, Degenstein L, Wise B, Fuchs E. The magical touch: genome targeting in epidermal stem cells induced by tamoxifen application to mouse skin. Proc Natl Acad Sci U S A 1999;96:8551–8556
23. McKay IA, Leigh IM. Epidermal cytokines and their roles in cutaneous wound healing. Br J Dermatol 1991;124:513–518
24. Aliahmadi E, Gramlich R, Grützkau A, et al. TLR2-activated human langerhans cells promote Th17 polarization via IL-1beta, TGF-beta and IL-23. Eur J Immunol 2009;39:1221–1230
25. Monsuur HN, Boink MA, Weijers EM, et al. Methods to study differences in cell mobility during skin wound healing in vitro. J Biomech 2016;49:1381–1387
26. Nicotera P, Melino G. Caspase-14 and epidermis maturation. Nat Cell Biol 2007;9:621–622
27. Zhao B, Qi Z, Li Y, Wang C, Fu W, Chen YG. The non-muscle-myosin-II heavy chain Myh9 mediates colitis-induced epithelium injury by restricting Lgr5+ stem cells. Nat Commun 2015;6:7166
28. Murthy A, Shao YW, Narala SR, Molyneux SD, Zúñiga-Pflücker JC, Khokha R. Notch activation by the metalloproteinase ADAM17 regulates myeloproliferation and atopic barrier immunity by suppressing epithelial cytokine synthesis. Immunity 2012;36:105–119
29. Winter M, Moser MA, Meunier D, et al. Divergent roles of HDAC1 and HDAC2 in the regulation of epidermal development and tumorigenesis. EMBO J 2013;32:3176–3191
30. Carter WG, Ryan MC, Gahr PJ. Epiligrin, a new cell adhesion ligand for integrin alpha 3 beta 1 in epithelial basement membranes. Cell 1991;65:599–610
31. Goldfinger LE, Hopkinson SB, deHart GW, Collawn S, Couchman JR, Jones JC. The alpha3 laminin subunit, alpha6beta4 and alpha3beta1 integrin coordinately regulate wound healing in cultured epithelial cells and in the skin. J Cell Sci 1999;112:2615–2629
32. Frank DE, Carter WG. Laminin 5 deposition regulates keratinocyte polarization and persistent migration. J Cell Sci 2004;117:1351–1363
33. Kim JM, Park WH, Min BM. The PPFLMLLKGSTR motif in globular domain 3 of the human laminin-5 alpha3 chain is crucial for integrin alpha3beta1 binding and cell adhesion. Exp Cell Res 2005;304:317–327
34. Sehgal BU, DeBiase PJ, Matzno S, et al. Integrin beta4 regulates migratory behavior of keratinocytes by determining laminin-332 organization. J Biol Chem 2006;281:35487–35498
35. Caruso R, Botti E, Sarra M, et al. Involvement of interleukin-21 in the epidermal hyperplasia of psoriasis. Nat Med 2009;15:1013–1015
36. Drake JM, Barnes JM, Madsen JM, Domann FE, Stipp CS, Henry MD. ZEB1 coordinately regulates laminin-332 and beta4 integrin expression altering the invasive phenotype of prostate cancer cells. J Biol Chem 2010; 285:33940–33948
37. Haensel D, Sun P, MacLean AL, et al. An Ovol2-Zeb1 transcriptional circuit regulates epithelial directional migration and proliferation. EMBO Rep 2019;20:e46273
38. Abshire CF, Carroll JL, Dragoi AM. FLASH protects ZEB1 from degradation and supports cancer cells' epithelial-to-mesenchymal transition. Oncogenesis 2016;5:e254
39. Reynolds LE, Conti FJ, Silva R, et al. alpha3beta1 integrin-controlled Smad7 regulates reepithelialization during wound healing in mice. J Clin Invest 2008;118:965–974
40. He Y, Thriene K, Boerries M, et al. Constitutional absence of epithelial integrin α3 impacts the composition of the cellular microenvironment of ILNEB keratinocytes. Matrix Biol 2018;74:62–76
41. McLean WH, Irvine AD, Hamill KJ, et al. An unusual N-terminal deletion of the laminin alpha3a isoform leads to the chronic granulation tissue disorder laryngo-onycho-cutaneous syndrome [published correction appears in Hum Mol Genet 2004;13:365]. Hum Mol Genet 2003;12:2395–2409
42. Kim KK, Wei Y, Szekeres C, et al. Epithelial cell alpha3beta1 integrin links beta-catenin and Smad signaling to promote myofibroblast formation and pulmonary fibrosis. J Clin Invest 2009;119:213–224
43. Watanabe M, Terasawa M, Miyano K, et al. DOCK2 and DOCK5 act additively in neutrophils to regulate chemotaxis, superoxide production, and extracellular trap formation. J Immunol 2014;193:5660–5667
44. Singh K, Sinha M, Pal D, et al. Cutaneous epithelial to mesenchymal transition activator ZEB1 regulates wound angiogenesis and closure in a glycemic status-dependent manner. Diabetes 2019;68:2175–2190
45. Tatari MN, De Craene B, Soen B, et al. ZEB2-transgene expression in the epidermis compromises the integrity of the epidermal barrier through the repression of different tight junction proteins. Cell Mol Life Sci 2014;71:3599–3609
46. Xu M, Zhu C, Zhao X, et al. Atypical ubiquitin E3 ligase complex Skp1-Pam-Fbxo45 controls the core epithelial-to-mesenchymal transition-inducing transcription factors. Oncotarget 2015;6:979–994
47. Chen A, Wong CS, Liu MC, et al. The ubiquitin ligase Siah is a novel regulator of Zeb1 in breast cancer. Oncotarget 2015;6:862–873
48. Zheng X, Narayanan S, Sunkari VG, et al. Triggering of a Dll4-Notch1 loop impairs wound healing in diabetes. Proc Natl Acad Sci U S A 2019;116: 6985–6994
49. Eckert RL, Efimova T, Dashti SR, et al. Keratinocyte survival, differentiation, and death: many roads lead to mitogen-activated protein kinase. J Investig Dermatol Symp Proc 2002;7:36–40
50. Ozawa K, Kondo T, Hori O, et al. Expression of the oxygen-regulated protein ORP150 accelerates wound healing by modulating intracellular VEGF transport. J Clin Invest 2001;108:41–50
51. Lim CH, Sun Q, Ratti K, et al. Hedgehog stimulates hair follicle neogenesis by creating inductive dermis during murine skin wound healing. Nat Commun 2018;9:4903
52. Sullivan SR, Underwood RA, Sigle RO, et al. Topical application of laminin-332 to diabetic mouse wounds. J Dermatol Sci 2007;48:177–188
53. Chang HY, Singh S, Mansour O, Baksh S, Alexander GC. Association between sodium-glucose cotransporter 2 inhibitors and lower extremity amputation among patients with type 2 diabetes. JAMA Intern Med 2018;178: 1190–1198
54. Nagae K, Uchi H, Morino-Koga S, Tanaka Y, Oda M, Furue M. Glucagon-like peptide-1 analogue liraglutide facilitates wound healing by activating PI3K/Akt pathway in keratinocytes. Diabetes Res Clin Pract 2018;146:155–161
55. Long M, Rojo de la Vega M, Wen Q, et al. An essential role of NRF2 in diabetic wound healing. Diabetes 2016;65:780–793
56. El-Sayed Moustafa JS, Eleftherohorinou H, de Smith AJ, et al. Novel association approach for variable number tandem repeats (VNTRs) identifies DOCK5 as a susceptibility gene for severe obesity. Hum Mol Genet 2012;21: 3727–3738